Effect of substrate bias on the structure and properties of multi-element (AlCrTaTiZr)N coatings

2006 J. Phys. D: Appl. Phys. 39 4628

(http://iopscience.iop.org/0022-3727/39/21/019)

INSTITUTE OF PHYSICS PUBLISHING JOURNAL OF PHYSICS D: APPLIED PHYSICS
J. Phys. D: Appl. Phys. **39** (2006) 4628–4633 doi:10.1088/0022-3727/39/21/019

Effect of substrate bias on the structure and properties of multi-element (AlCrTaTiZr)N coatings

Chia-Han Lai, Su-Jien Lin, Jien-Wei Yeh and Andrew Davison

Department of Materials Science and Engineering, National Tsing Hua University, Hsinchu 300, Taiwan, Republic of China

Received 17 July 2006, in final form 28 August 2006
Published 20 October 2006
Online at stacks.iop.org/JPhysD/39/4628

Abstract
Multi-element (AlCrTaTiZr)N coatings are prepared by reactive RF magnetron sputtering. The influence of substrate bias (0 to −200 V) on the deposition rate, composition, structure and mechanical properties of these coatings is investigated. A reduction in both deposition rate and Al concentration is observed with increasing substrate bias. The grounded substrate is found to possess a columnar structure. The columnar structure is not so apparent in the denser coatings deposited at an applied substrate bias of −150 V. Furthermore, a minimum in coating roughness is found to occur at the intermediate substrate bias of −100 V. All the (AlCrTaTiZr)N coatings appear to have a single FCC structure from XRD analysis. Furthermore, it is determined from XRD that there is an increase in both (111) peak intensity and grain size, and a decrease in the lattice strain, for increasing substrate bias. The residual stress, hardness, elastic modulus and toughness of the coatings are found to be greatly enhanced by the substrate bias. The highest hardness and elastic modulus of approximately 36 Gpa and 360 GPa, respectively, were obtained at a substrate bias of −150 V.

1. Introduction

A surface coating is an effective method for improving the durability of materials used in aggressive environments. By properly selecting the coating method and materials, the service life of a component may be prolonged significantly and its commercial value increased [1]. For many years binary transition metal nitrides, owing to their good mechanical and thermal properties, have been used as protective coatings [2]. These simple nitrides, however, have now been surpassed by more complex ternary systems, for example, the development of the ternary TiAlN system which provides enhanced hardness and/or oxidation resistance over its TiN binary counterpart [2]. At present, the majority of work on coatings has been limited to ternary or quaternary systems [2–4].

Recently, Yeh *et al* proposed a novel bulk alloy design that consists of five or more principal elements in near equimolar ratio [5]. These alloys, referred to as 'high-entropy alloys' (HEAs), have been found to develop simple solid-solution structures with uniformly distributed nanoscale precipitates and possess as-cast hardnesses up to HV 850 [5–7]. Moreover, these high as-cast hardnesses were even found to be retained after thermal annealing at 1000 °C for 12 h. HEAs have also been found to exhibit high strength and good fatigue resistance in high-temperature water environments [6, 7]. Based on these bulk properties, consideration has been made towards the deposition from HEA targets not only to produce multi-component nitride, carbide, boride or oxide coatings that may retain many of the beneficial attributes of the bulk alloys, but also to exhibit some superior qualities, such as a greatly increased hardness. From initial studies of multi-element nitride coatings, prepared by reactive magnetron sputtering, it was found that the maximum hardness attained, however, was only 15 GPa [8, 9]. The high content of non-nitride forming elements within these coatings may be the reason for the low hardness of these previously deposited nitride coatings.

Thus, in the present work, nitride films comprising a number of nitrogen affinitive transition metal elements, i.e. AlCrTaTiZr, shall be examined. The coatings will be deposited by reactive RF magnetron sputtering from a single equiatomic AlCrTaTiZr target. The substrate bias, known to be a significant factor influencing coating properties [10], shall

be varied, and the related changes in microstructure, film topography, and mechanical properties examined.

2. Experimental

2.1. Film preparation

An AlCrTaTiZr alloy target, with each element in equiatomic proportion, was prepared by vacuum arc melting. After repeatedly melting the target material at least five times to improve its chemical homogeneity, it was cut and polished into a disc 50 mm in diameter. The AlCrTaTiZr nitride films were deposited onto silicon wafers by reactive RF magnetron sputtering operated at a target power of 150 W. The base pressure of the deposition chamber was better than 1×10^{-3} Pa. The working pressure was fixed at 0.8 Pa in a 50 : 50 Ar : N_2 ratio with a total gas flow of 60 sccm. The substrates were heated to 623 K prior to deposition. A DC bias from 0 to −200 V was applied to the substrates. The thickness of the nitride films was fixed at 1.3 μm by adjusting the deposition time.

2.2. Film characterization

The crystallographic structures of the films were characterized using glancing angle x-ray diffraction (GAXRD, Rigaku D/MAX2500) with Cu–Kα radiation and an incident angle of 2°. The surface and cross-section of the coatings were observed by scanning electron microscopy (SEM, JEOL JSM 5410 and 6500F). Atomic force microscopy (AFM, Digital Instrument NS3a Controller with the D3100 Stage) was used to evaluate coating topography and root-mean-squared (RMS) roughness. The chemical composition of the AlCrTaTiZr HEA target and the nitride coatings were analysed with an electron probe microanalyzer (EPMA, JEOL JAX-8800). The residual stress was determined by the substrate-curvature technique using Stoney's equation [10]. The hardness and modulus of these nitride coatings were measured by a nanoindenter (XP nanomechanical testing system, MTS Corporation) using a Berkovich indenter and a continuous applied load of 8 mN. The penetration depth of the indenter was controlled to be less than 10% of the film thickness in order to limit the influence of the substrate [11]. The toughness was interpreted from a Vickers indentation (Mitutoyo HM-115) performed at a load of 100 g and held for 15 s.

3. Results and discussion

3.1. Deposition rate, surface morphology and cross-sectional microstructure

Figure 1 shows the deposition rate of the multi-element (AlCrTaTiZr)N coatings as a function of substrate bias (V_s). Due to densification and resputtering of the coating material [12], the deposition rate is seen to decrease gradually from 14 to 11 nm min^{-1} with increasing substrate bias. This increase in densification and resputtering of the coating is expected to result from an increase in the energy of the ions (U_k) bombarding the growing film, which can be related to the other

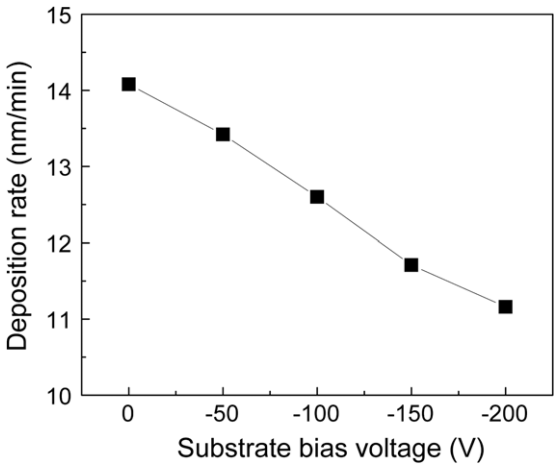

Figure 1. Deposition rate as a function of substrate bias.

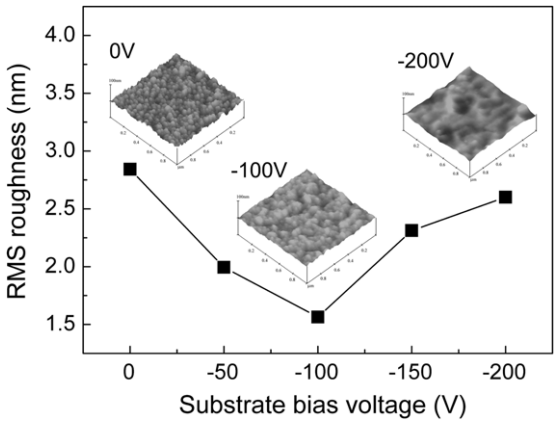

Figure 2. AFM surface roughness and morphology of the (AlCrTaTiZr)N coatings deposited at different substrate biases.

process parameters by the following [13]:

$$U_k \propto \frac{D_w V_s}{P_g^{0.5}},$$

where, D_w is the target power density and P_g is the process pressure. Therefore, as D_w and P_g are maintained constant, the above expression indicates that U_k is directly proportional to V_s.

Figure 2 shows the RMS roughnesses of the multi-element (AlCrTaTiZr)N coatings, along with the AFM surface morphologies of the films deposited at substrate biases of 0, −100 and −200 V. When the substrate is grounded, i.e. 0 V, the (AlCrTaTiZr)N coatings exhibit a cauliflower-like surface with a large roughness of 2.54 nm. As the voltage is increased, there is initially a decrease in the roughness, with a minimum of 1.56 nm occurring at −100 V, beyond which the roughness again increases, reaching 2.60 nm at −200 V. The cauliflower-like surface and higher roughness of the coating deposited at 0 V is attributed to the energy of the bombarding ions being insufficient to promote appreciable surface mobility of the ad-atoms along with self-shadowing effects. This is in agreement with the proposed structure zone model of Messier [14]. The lower surface roughness at −100 V is attributed to increased surface diffusion, sputtering and densification of the coating material by higher energy ions [15]. Ion induced damage is

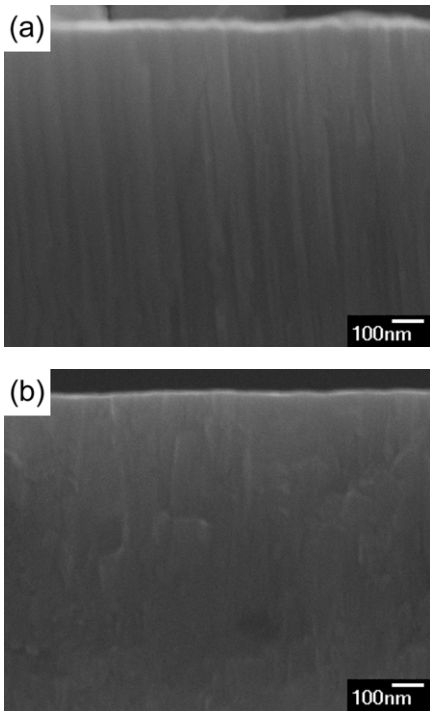

Figure 3. Cross-sectional SEM micrographs of the AlCrTaTiZrN coatings deposited at substrate bias of (*a*) 0 V and (*b*) −150 V.

considered the reason for the increase in the roughness at biases greater than −100 V.

Figures 3(*a*) and (*b*) shows the cross-sectional SEM micrographs for the coatings deposited at 0 V and −150 V, respectively. The grounded coating (figure 3(*a*)) shows a clear columnar structure. The biased coating (figure 3(*b*)) appears more dense with a less defined columnar structure. As discussed in the case of roughness above, the increased ion bombardment induced surface diffusion and sputtering of the coating material is considered to result in a higher density of the biased coating; such results have been reported for other nitride coatings deposited at higher substrate biases [16].

3.2. Chemical composition

The target is found to have a virtually equiatomic composition of $Al_{0.20}Cr_{0.20}Ta_{0.19}Ti_{0.19}Zr_{0.22}$. The concentration of the various elements in the (AlCrTaTiZr)N coatings as a function of substrate bias is shown in figure 4. The N content is seen to be almost independent of the substrate bias. The concentration of Al is decreased with increasing applied voltage, thus resulting in an increase in the other target elements. The reduced Al content is attributed to its higher sputtering yield than the other elements present [17].

3.3. XRD analysis

XRD patterns of the AlCrTaTiZr alloy target and its nitride coatings deposited at different substrate biases are presented in figure 5. The alloy target is obtained as a simple bcc solid-solution phase and as an Al_2 Zr compound. The (1 1 1), (2 0 0), (2 2 0), and (3 1 1) peaks of the (AlCrTaTiZr)N are indexed as

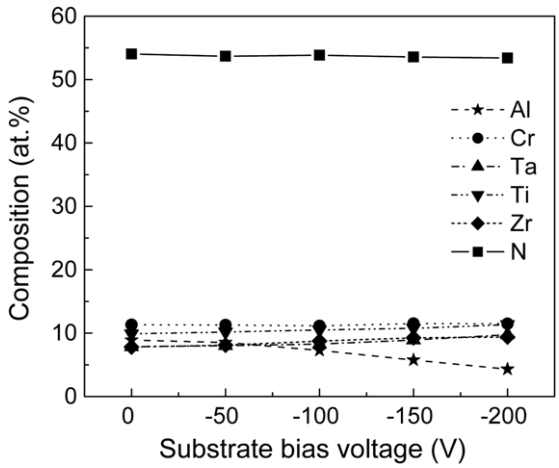

Figure 4. EPMA determined concentration of the various elements present within the (AlCrTaTiZr)N coatings as a function of substrate bias.

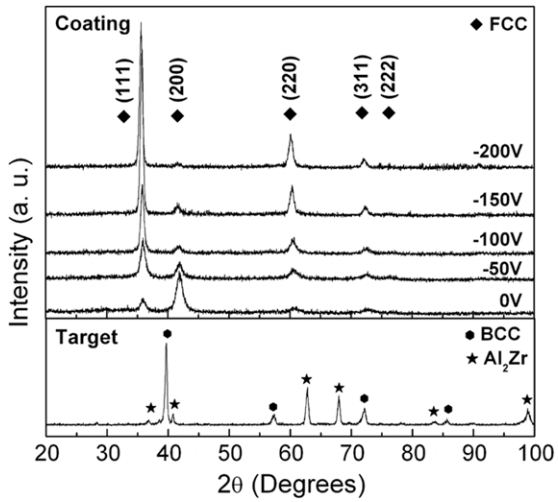

Figure 5. XRD patterns of the AlCrTaTiZr alloy target and its nitride coatings deposited at different substrate voltages.

belonging to an FCC structure of the B1 phase (NaCl-type). The lattice parameters of these coatings, further evaluated from the XRD patterns, are found to increase from 0.430 to 0.435 nm with an increase in substrate bias. Since in the XRD pattern of the (AlCrTaTiZr)N coating only one group of peak revealing the FCC structure is observed, indicating this coating tends to form a single solid-solution nitride phase rather than the co-existence of separated nitrides. This is in agreement with our previous studies [18]. A single FCC solid-solution nitride phase in ternary and quaternary nitride coating systems has also been reported in the other literature [19,20]. A shift of the XRD peaks to lower angles is observed with increasing substrate bias. This agrees well with an increase in the lattice parameters of the (AlCrTaTiZr)N coatings as mentioned above, and is considered to result, in part, from the substitution of Al atoms by elements of larger atomic radii. Such an increase in lattice spacing was previously reported for (TiCrAl)N coatings as the aluminium content decreased [21]. As a result of energized ion bombardment, the well-known atomic peening effect is an additional factor that can expand the interplanar spacing [10].

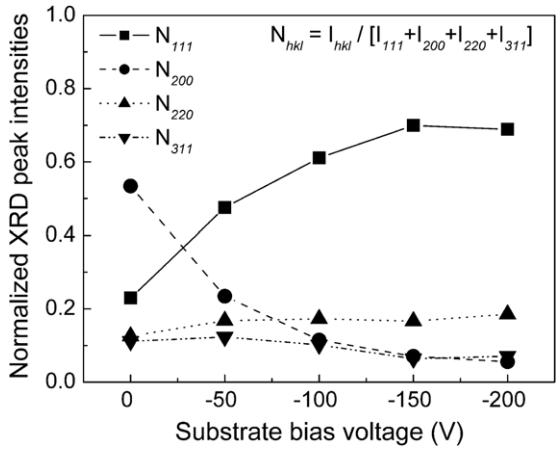

Figure 6. The dependence of the normalized *hkl* XRD peak intensities, N_{hkl} ($I_{hkl}/[I_{111}+I_{200}+I_{220}+I_{311}]$), of the (AlCrTaTiZr)N coatings as a function of substrate bias.

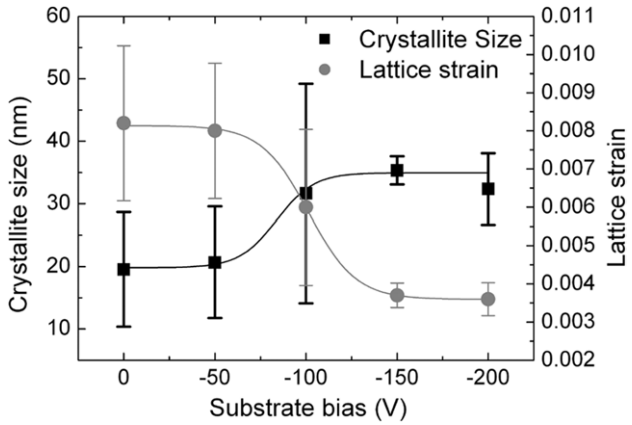

Figure 7. The crystallite size and lattice strain of (AlCrTaTiZr)N coatings as a function of substrate bias.

From an examination of the peak intensities in figure 6, the results clearly demonstrate that the substrate bias greatly influences the orientation of the coatings. It has been stated that the preferred orientation of thin films with a NaCl-type structure is determined by the competition between the surface and strain energy [22]. Therefore, as the (2 0 0) and (1 1 1) planes, respectively, have the lowest surface and strain energies for the NaCl-type crystal structure [22], the preferential (1 1 1) orientation at the higher applied bias is considered to develop in order to reduce the increased strain energy resulting from the more energetic impinging ions.

The crystallite size and lattice strain, estimated from broadening of the XRD peaks according to the Williamson–Hall method [23], are presented in figure 7. Four diffraction peaks ((1 1 1), (2 0 0), (2 2 0) and (3 1 1)) are considered in the present study. It is found that the crystallite size increases and the lattice strain decreases with increasing substrate bias. The large error bars as revealed in figure 7 are mainly attributed to the larger inaccuracy in determining broadening of some XRD peaks with weaker intensities (e.g. (2 0 0) at higher bias and (3 1 1) at lower bias). In general, the crystallite size has been found to decrease with the increase in substrate bias due to the continuous renucleation of growing films induced by the ion-

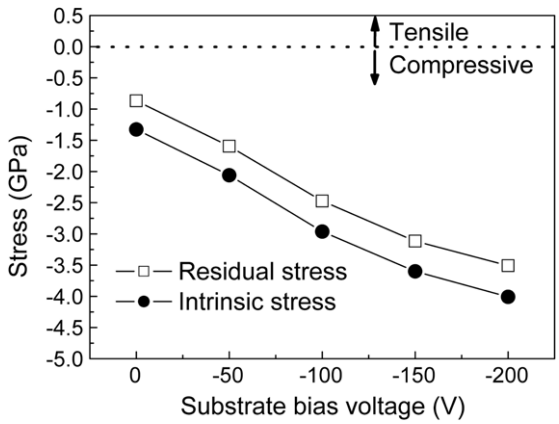

Figure 8. The residual stress of the (AlCrTaTiZr)N coatings as a function of substrate bias.

irradiation-generated defects [24]. Nevertheless, the opposite tendency is observed in the present study, i.e. the crystallite size increases with the increase in substrate bias. This result is also in agreement with TiN coatings obtained by Espinoza-Beltran *et al* [25]. However, the exact correlation between crystallite size, lattice strain and substrate bias is not known so far and further detailed study accounting for this result is still needed.

3.4. Mechanical properties

The coatings all possess a compressive residual stress that increases from −0.9 to −3.5 GPa with substrate bias, as shown in figure 8. The measured residual stress of the coatings is composed principally of two components, these being the thermal stress (σ_{th}) and the intrinsic stress (σ_{in}). The thermal stress, which results from the differences in the coefficient of thermal expansion (CTE) between the coating and the substrate, can be estimated from the following equation [26]:

$$\sigma_{\mathrm{th}} = \Delta\alpha \cdot \Delta T \frac{E_{\mathrm{f}}}{(1-\upsilon_{\mathrm{f}})},$$

where, $\Delta\alpha$ is the difference in CTE between the substrate and coating, ΔT is the difference between the temperature during deposition and that at ambience, E_{f} and υ_{f} are the elastic modulus and Poisson's ratio of the coating, respectively. The (AlCrTaTiZr)N films are assumed to have a υ_{f} of 0.25, as this is typical of ceramic materials. The CTE of the Si substrate is 2.4×10^{-6} K^{-1} [27]. The overall CTE of the coatings is estimated from the rule of mixtures for the individual binary nitrides, i.e. $\alpha_{\mathrm{AlN}} = 5.7 \times 10^{-6}\,\mathrm{K}^{-1}$, $\alpha_{\mathrm{CrN}} = 2.3 \times 10^{-6}\,\mathrm{K}^{-1}$, $\alpha_{\mathrm{TaN}} = 3.6 \times 10^{-6}\,\mathrm{K}^{-1}$, $\alpha_{\mathrm{TiN}} = 9.4 \times 10^{-6}\,\mathrm{K}^{-1}$ and $\alpha_{\mathrm{ZrN}} = 7.2 \times 10^{-6}\,\mathrm{K}^{-1}$, [27,28] using the EPMA determined elemental concentrations shown in figure 2. The elastic moduli of the coatings are shown in figure 9(*b*). The thermal stress is estimated to be tensile in the range 0.46–0.50 GPa. However, as the temperature is held constant and the compositional changes are small (figure 4), the change in the residual stress of the deposited coatings is mainly a result of the increasing intrinsic stress, as shown in figure 8. These intrinsic stresses are considered to originate from the well-known atomic peening effect [10, 29], whereby the impinging ions knock surface atoms deeper into the film, where they become trapped. The

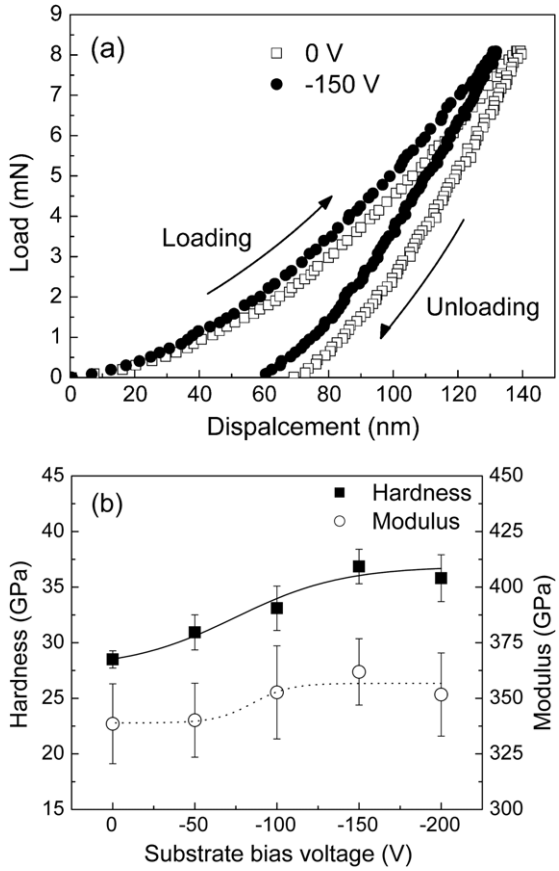

Figure 9. (*a*) Typical nanoindentation loading-unloading curves of multi-element (AlCrTaTiZr)N films deposited at 0 V and −150 V, (*b*) hardness and modulus of these nitride films as a function of substrate bias.

shift of the XRD peaks to lower angles, as shown in figure 3, is also likely to result somewhat from this increase in compressive stress.

The typical loading–unloading curves during nanoindentation of the multi-element (AlCrTaTiZr)N coatings deposited at 0 and −150 V are shown in figure 9(*a*). The hardness and elastic modulus of these multi-element coatings are shown in figure 9(*b*). The hardness and elastic modulus increase to maximum values of about 36 Gpa and 360 GPa, respectively, at a substrate bias of −150 V. There are numerous factors that may affect the measured hardness of these coatings, including the crystallite size, preferred orientation, residual stress and densification of coatings. It is found that beyond a critical crystallite size, generally approximately 10 nm, materials tend to follow the Hall–Petch relationship, i.e. the hardness decreases with an increase in crystallite size [30]. However, in the present study the opposite occurs, i.e. the hardness of (AlCrTaTiZr)N coatings increases as the grain size increases from about 20 to 34 nm (refer to figure 7). This suggests that crystallite size is not the dominant factor for the hardness of the present coatings. For other FCC nitrides, i.e. TiN and ZrN, it has been found that the coatings with a preferred (1 1 1) orientation possess the highest hardness [31,32]. The increased (1 1 1) orientation of the present FFC (AlCrTaTiZr)N coatings deposited at higher substrate biases may therefore be the reason for the higher hardness. Moreover, the increase in compressive residual stress and density with substrate bias will be expected to increase the measured hardness.

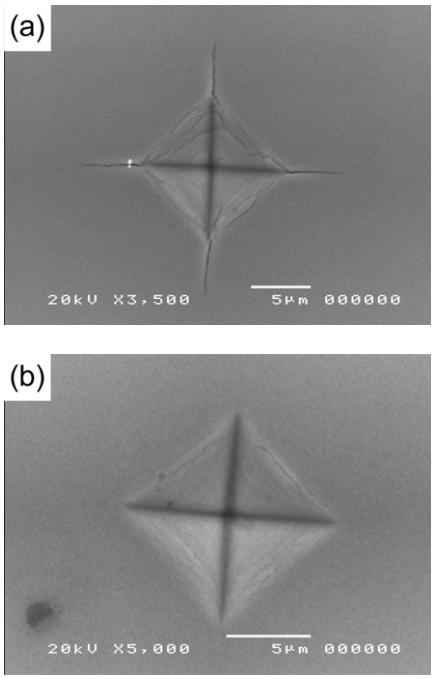

Figure 10. SEM micrographs of the Vickers indentations made at a normal load of 100 g into the (AlCrTaTiZr)N coatings deposited at (*a*) 0 V and (*b*) −150 V.

Toughness, i.e. the resistance of a material to prevent the formation and propagation of cracks, is another important coating property. The plane-view SEM images of the Vickers indentations made in the 0 and −150 V coatings are shown in figure 10. By the fact that it shows very insignificant crack formation, the coating deposited at a substrate bias of −150 V shows a greatly improved toughness compared with that deposited at 0 V. Since cracking is generally initiated by tensile stresses, any residual compressive stress of a thin film has to be overcome first [33], and this can to a great extent explain the improved toughness of the coating deposited at −150 V. The higher density of the (AlCrTaTiZr)N coatings deposited at the higher substrate bias may provide additional enhancement to its toughness [34].

4. Conclusions

From the deposition of (AlCrTaTiZr)N coatings by reactive RF magnetron sputtering onto differently biased substrates, the following were found.

(i) There was a reduction in the deposition rate and the Al content with increasing substrate bias.
(ii) The lowest roughness of 1.56 nm was obtained at a substrate bias of −100 V.
(iii) An increase in bias was found to result in the less defined column structure with higher density.
(iv) The deposited (AlCrTaTiZr)N coatings possessed a single FCC solid-solution structure. The lattice expanded at higher substrate biases as a result of the depletion in the Al content and the ion peening effect.

(v) The preferred crystallographic orientation changed from (2 0 0) to (1 1 1) with increasing substrate bias. Moreover, the compressive intrinsic stresses increased with the voltage applied to the substrate.

(vi) The increase in hardness and elastic modulus of (AlCrTaTiZr)N, with maxima of 36 GPa and 360 GPa, respectively, at a substrate bias of −150 V, was considered a synergistic effect of the preferred (1 1 1) orientation, greater compressive stress and denser coatings formed at higher voltages.

(vii) Toughness for the coating biased at −150 V was significantly improved to that deposited on the grounded substrate.

Acknowledgments

The authors are pleased to acknowledge financial support for this research given by The National Science Council of Taiwan, under Grant No NSC-94-2120-M-007-007.

References

[1] Sproul W D 1996 *Science* **273** 889
[2] PalDey S and Deevi S C 2003 *Mater. Sci. Eng.* A **342** 58
[3] Lee D K, Kang D S, Suh J H, Park C-G and Kim K H 2005 *Surf. Coat. Technol.* **200** 1489
[4] Yamamoto K, Sato T, Takahara K and Hanaguri K 2003 *Surf. Coat. Technol.* **174–175** 620
[5] Yeh J W, Chen S K, Lin S J, Gan J Y, Chin T S, Shun T T, Tsau C H and Chang S Y 2004 *Adv. Eng. Mater.* **6** 299
[6] Chen Y Y, Duval T, Hung U D, Yeh J W and Shih H C 2005 *Corros. Sci.* **47** 2257
[7] Chen Y Y, Hong U T, Yeh J W and Shih H C 2005 *Appl. Phys. Lett.* **87** 261918
[8] Chen T K, Shun T T, Yeh J W and Wong M S 2004 *Surf. Coat. Technol.* **188–89** 193
[9] Chen T K, Wong M S, Shun T T and Yeh J W 2005 *Surf. Coat. Technol.* **200** 1361
[10] Bull S J, Jones A M and McCabe A R 1992 *Surf. Coat. Technol.* **54** 173
[11] Bull S J 2005 *J. Phys. D: Appl. Phys.* **38** R393
[12] Lee M K, Kang H S, Kim W W, Kim J S and Lee W J 1997 *J. Mater. Res.* **12** 2393
[13] Zhang S, Sun D, Fu Y Q, Du H J and Zhang Q 2004 *Diamond Relat. Mater.* **13** 1777
[14] Messier R, Venugopal V C and Sunal P D 2000 *J. Vac. Sci. Technol.* A **18** 1538
[15] Muller K H 1987 *Phys. Rev.* B **35** 7906
[16] Park H S, Jung D H, Na H D, Joo J H and Lee J J 2001 *Surf. Coat. Technol.* **142** 999
[17] Mahan J E 2000 *Physical Vapor Deposition of Thin Films* (New York: Wiley)
[18] Lai C H, Lin S J, Yeh J W and Chang S Y 2006 *Surf. Coat. Technol.* at press
[19] Lamni R, Sanjines R, Parlinska-Wojtan M, Karimi A and Levy F 2005 *J. Vac. Sci. Technol.* A **23** 593
[20] Kathrein M, Michotte C, Penoy M, Polcik P and Mitterer C 2005 *Surf. Coat. Technol.* **200** 1867
[21] Yamamoto K, Sato T, Takahara K and Hanaguri K 2003 *Surf. Coat. Technol.* **174** 620
[22] Pelleg J, Zevin L Z, Lungo S and Croitoru N 1991 *Thin Solid Films* **197** 117
[23] Williamson G K and Hall W H 1953 *Acta. Mater.* **1** 22
[24] Hakansson G, Sundgren J E, McIntyre D, Greene J E and Munz W D 1987 *Thin Solid Films* **153** 55
[25] Espinoza-Beltran F J, Che-Soberanis O, Garcia-Gonzalez L and Morales-Hernandez J 2003 *Thin Solid Films* **437** 170
[26] Bendavid A, Martin P J, Wang X, Wittling M and Kinder T J 1995 *J. Vac. Sci. Technol.* A **13** 1658
[27] Kadoshima M, Akiyama K, Yamamoto K, Fujiwara H, Yasuda T, Nabatame T and Toriumi A 2005 *J. Vac. Sci. Technol.* B **23** 42
[28] Holleck H 1986 *J. Vac. Sci. Technol.* A **4** 2661
[29] Oettel H and Wiedemann R 1995 *Surf. Coat. Technol.* **76** 265
[30] Veprek S 1999 *J. Vac. Sci. Technol.* A **17** 2401
[31] Huang J H, Tsai Y P and Yu G P 1999 *Thin Solid Films* **356** 440
[32] Chou W J, Yu G P and Huang J H 2002 *Thin Solid Films* **405** 162
[33] Zhang S, Sun D, Fu Y Q and Du H J 2005 *Surf. Coat. Technol.* **198** 2
[34] Chen C S, Liu C P, Yang H G and Tsao C Y A 2004 *J. Vac. Sci. Technol.* A **22** 2041